Optic Radiations Microstructural Changes in Glaucoma and Association With Severity: A Study Using 3Tesla-Magnetic Resonance Diffusion Tensor Imaging

Laury Tellouck, Muriel Durieux, Pierrick Coupé, Audrey Cougnard-Grégoire, Joy Tellouck, Thomas Tourdias, Fanny Munsch, Arnaud Garrigues, Catherine Helmer, Florence Malet, et al.

HAL Id: hal-01456234

https://hal.science/hal-01456234

Submitted on 4 Feb 2017

1 **OPTIC RADIATIONS MICROSTRUCTURAL CHANGES IN**

2 **GLAUCOMA AND ASSOCIATION WITH SEVERITY: A STUDY USING**

3 **3TESLA-MAGNETIC RESONANCE DIFFUSION TENSOR IMAGING**

4
5
6

7 Laury Tellouck[1,2,3], Muriel Durieux [4], Pierrick Coupé [5,6], Audrey Cougnard-Grégoire[2,3],

8 Joy Tellouck[1], Thomas Tourdias [2,4,7], Fanny Munsch [4]; Arnaud Garrigues [1], Catherine

9 Helmer [2,3], Florence Malet[8], Jean-François Dartigues [2,3], Vincent Dousset [2,4,7], Cécile

10 Delcourt[2,3], Cédric Schweitzer[1,2,3]

11
12
13

14 1: CHU de Bordeaux, Service d'Ophtalmologie, F-33000 Bordeaux, France.

15 2: Univ. Bordeaux, F-33000 Bordeaux, France.

16 3: INSERM, U1219 - Bordeaux Population Health Research Center, F-33000

17 Bordeaux, France.

18 4: CHU de Bordeaux, Service de Neuro-Imagerie, F-33000 Bordeaux, France.

19 5: Université de Bordeaux, LaBRI, UMR 5800, PICTURA, F-33400 Talence, France.

20 6: CNRS, LaBRI, UMR 5800, PICTURA, F-33400 Talence, France.

21 7 : INSERM U1215, Neurocentre Magendie, F-33000 Bordeaux, France.

22 8: Centre d'Ophtalmologie Point Vision, F-33000 Bordeaux, France.

23
24
25

26 Corresponding author/reprint request: Cécile Delcourt, Inserm U1219, ISPED, 146

27 rue Léo Saignat, 33076 Bordeaux Cedex. Tel: + 33 557 57 11 91. Email:

28 cecile.delcourt@isped.fr

29

30 Word count: 4089

35
36
37

ABSTRACT

Purpose:

To compare microstructural changes along the optical radiations and brain structure volumes between glaucoma and control subjects using in vivo magnetic resonance imaging and to analyze their association with severity of the disease.

Methods: 50 open-angle glaucoma subjects and 50 healthy age- and sex-matched controls underwent detailed ophthalmological examinations (including visual field testing (VF), funduscopy and Spectral-Domain Optical Coherence Tomography) as well as Diffusion tensor imaging (DTI) using a 3.0-Tesla MRI. Fractional anisotropy (FA), Mean Diffusivity, Radial Diffusivity (RD) and Axial Diffusivity (AD) were quantified semi-automatically along the optical radiations. DTI parameters and volumes of specific brain structures were compared between cases and controls using conditional logistic regression. Association between DTI metrics and the severity of the disease was studied using linear mixed regression analyses.

Results: In glaucoma subjects, optic radiations FA was significantly lower (0.57 vs 0.59; p= 0.02) and RD was significantly higher (52.78 10^{-5} mm^2/s vs 49.74 10^{-5} mm^2/s; p= 0.03) than in controls. Optic radiations FA was significantly correlated with homolateral functional and structural damage of glaucoma (mean deviation of VF (p=0.03), retinal nerve fiber layer thickness (p=0.03), vertical cup/disc ratio (p=0.0007)). Volume and DTI parameters of other brain structures (including hippocampus) were not significantly different between glaucoma and controls.

Conclusion: We evidenced microstructural modifications along visual pathways of glaucoma patients and these alterations were correlated with disease severity. The association of glaucoma with other neurodegenerative alterations would need further exploration and a prospective follow-up of our cohort of subjects.

Keywords: glaucoma, fractional anisotropy, 3T MRI, optic radiations, DTI

68
69 **INTRODUCTION**
70
71
72 Glaucoma affects 64 million people and is the first cause of irreversible blindness,

73 worldwide[1,2]. It encompasses a group of disorders characterized by progressive

74 degeneration of the optic nerve head, loss of retinal ganglion cells and a

75 corresponding pattern of visual field loss[3]. Primary open-angle glaucoma (POAG) is

76 the predominant form of glaucoma in Western countries. Although some risk factors

77 for POAG have been identified (high intraocular pressure, age, high myopia, ethnicity

78 and heredity), several aspects of its pathophysiology remain unclear. As the disease

79 could also affect intra-cerebral visual pathways in addition to optic nerve head

80 degeneration, a neurodegenerative hypothesis raises concerns[4,5]

81 Central visual pathway degeneration in glaucoma was first suggested in experimental

82 and histological studies, which have evidenced that glaucoma is not strictly limited to

83 the optic nerve[6,7]. In an animal model of ocular hypertension, brain changes were

84 observed in the lateral geniculate nucleus and superior colliculus, in parallel with

85 retinal ganglion cells loss[8]. In another study, grey matter of glaucoma patients was

86 reduced compared to healthy subjects, in the approximate retinal lesion projection

87 zones in the visual cortex[9]. Moreover, a clinicopathological case in humans

88 highlighted a neural degeneration in intracranial optic nerve, lateral geniculate

89 nucleus and visual cortex[10]. This paradigmatic shift is further supported by several

90 other small-sized clinical studies using brain magnetic resonance imaging, showing

91 reduced volume of all the visual pathways (optic tracts, optic chiasm, lateral

92 geniculate nucleus, optic radiations) measured at 1.5T[11–13] or 3T field strength[14,15].

93 Some other experimental studies may help understand the pathogenesis of the

94 disease. Using in vivo MRI studies is a way to study metabolic and spatiotemporal

95 changes in glaucoma[16–18].

96 In addition, epidemiological studies have also suggested that glaucoma might be

97 associated with other neurodegenerative disorders, in particular Alzheimer's

98 disease[19,20], and a few studies have found a reduced volume of brain structures,

99 beyond the visual pathways – particularly in the hippocampus – which is well known

100 to be affected in Alzheimer's disease[14,21,22]. These data have nevertheless been

101 collected in patients with long standing disease. Whether subtle alterations

102 suggestive of associated neurodegenerative disease can be captured from the early

103 stage of glaucoma, prior to atrophy, is unknown.

104 Recent improvements in neuroimaging techniques allow more accurate evaluation of

105 brain structure volumes and intra-cerebral microstructural damage. By quantifying

106 microscopic movements of water molecules, Diffusion Tensor Imaging (DTI) – a

107 functional MRI technique – provides a sensitive evaluation of underlying brain

108 microstructural changes even prior to atrophy[23]. Therefore, this technique appears

109 particularly promising in the documentation of intra-cerebral damage in glaucoma.

110 The most commonly assessed DTI parameters include fractional anisotropy (FA,

111 which reflects the degree of cellular structural alignment within fiber tracts and the

112 structural integrity of the fiber tracts) and mean diffusivity (MD, which measures the

113 average motion of water molecules independently of fiber directionality).

114

115 Several case-control studies have already shown that FA of the optic radiations is

116 decreased and MD increased in glaucoma patients[24,25], and some others have

117 suggested that these changes may be progressive with increasing axon loss of the

118 optic nerve[26]. Whereas these studies provide new insights in the understanding of

119 glaucoma disease, they were limited in sample size and mainly included advanced

120 glaucoma patients.

121

122 Therefore, our study aimed at exploring the potential neurodegenerative hypothesis

123 associated with glaucoma and whether subtle changes could be measurable at the

124 early stage of the disease. Thus we analyzed both the microstructural changes of the

125 visual pathway, in relation with glaucoma severity, as well as changes beyond the

126 visual pathway, in particular in regions affected in neurodegenerative pathologies.

127

128

129 **METHODS**

130

131 **Patient Population**

132 This study is an observational case-control study performed at the University Hospital

133 of Bordeaux. Fifty patients with POAG (20 men, 30 women, mean age 61.9 +/- 6.9

134 years) and 50 age- and sex-matched controls (20 men, 30 women, mean age 61.9 +/-

135 7.0 years) were prospectively included.

136 This research followed the tenets of the Declaration of Helsinki. Participants gave

137 written consent for the participation in the study. The design of this study was

138 approved by the Ethical Committee of Bordeaux (Comité de Protection des Personnes

139 Sud-Ouest et Outre-Mer III) in March 2012. This study was registered on the website

140 http://clinicaltrials.gov/ (identifier NCT01621841).

141

142 **Ophthalmological Examination**

143 All participants underwent a complete ophthalmic examination including measurement

144 of best-corrected visual acuity, intraocular pressure (IOP) using Goldmann aplanation

145   tonometry, gonioscopy, slit-lamp biomicroscopy and optic disc examination by

146   funduscopy. Central corneal thickness and anterior chamber depth were assessed

147   using interferometry (OCT Visante, Carl Zeiss Meditec, Inc., Dublin, CA, USA), and

148   axial length measurement using IOL Master (Carl Zeiss Meditec, Inc., Dublin, CA,

149   USA). All participants underwent a visual field testing (Octopus 101, Haag-Streit, Inc.,

150   Bern, Switzerland) and only reliable tests (false-positive errors <15%, false negative-

151   errors <15%, loss fixations <20%) were included. In addition, visual fields (VF) were

152   reviewed and excluded in the presence of artefacts, such as eyelid or rim artifacts,

153   fatigue effects, inattention, or inappropriate fixation.

154   A measurement of peripapillary Retinal Nerve Fiber Layer (RNFL) thickness was

155   performed using Spectral-Domain optical coherence tomography (SD-OCT) (Cirrus,

156   Carl Zeiss Meditec, Inc., Dublin, CA, USA). All images were acquired and reviewed by

157   specially trained technicians of the study to control the quality of signal strength and

158   accurate centration and segmentation of the RNFL circle scan acquisition. Signal

159   strength lower than 6 or acquisitions with artifacts were excluded from the analysis.

160   Glaucoma subjects and controls received a questionnaire requesting for

161   cardiovascular risk factors, familial history of glaucoma, ophthalmological diseases

162   and current medications. Each participant underwent Mini Mental State Examination

163   (MMSE)[27].

164

165   Primary open-angle glaucoma was defined by the following criteria: the presence of

166   glaucomatous optic neuropathy (defined as a loss of neuroretinal rim with a vertical

167   cup-to-disc ratio [VCDR] of >0.7 or an intereye asymmetry of >0.2, with or without

168   notching attributable to glaucoma) associated to compatible VF loss. This VF loss was

169   defined as the presence of at least 3 contiguous non edge test points within the same

170 hemifield on the pattern deviation probability plot at P < 0.05, with at least 1 point P <

171 0.01, excluding points directly above and below the blind spot, and the presence of

172 glaucomatous hemifield test results outside normal limits. Iridocorneal angle opening

173 was graded 3 or 4 on gonioscopy using Schaeffer classification.

174 Controls were defined as normal optic disc without notching or abnormal thinning of

175 the neuroretinal rim, no visual field defects, IOP measurement < 21 mmHg and no

176 family history of glaucoma.

177 Exclusion criteria included any diseases that could affect the visual field, secondary

178 glaucoma including exfoliative and pigmentary glaucoma, diabetes mellitus, any

179 neurological or psychiatric disorders, and a score <26 on the MMSE for global

180 cognition. We also excluded participants according to standard MRI exclusion criteria

181 such as claustrophobia, ferromagnetic implants or pacemakers, and inability to lie still

182 for the MRI acquisition time.

183 Stage of severity of glaucoma was classified according to the Hodapp-Parrish-

184 Anderson classification[28]. The different stages are:

185 - Stage 0: no or minimal defect

186 - Stage 1: MD ≥ -6.0 dB (early defect)

187 - Stage 2: -12.0 ≥ MD ≥ -6.0 dB (moderate defect)

188 - Stage 3: -20 ≥ MD ≥ -12.0 dB (advanced defect)

189 - Stage 4: MD ≥ - 20.0 dB (severe defect)

190 - Stage 5: End-stage disease

191

192

193 **MRI Data Acquisition**

194 MRI examinations were performed on a 3-T Discovery MR750w scanner (GE Medical

195 Systems, Milwaukee, WI, USA) using a 32-channel phased array head coil within 30

196 days following the ophthalmologic examinations. The protocol included a DTI

197 sequence to look for microstructural alterations along and beyond the optic radiations,

198 a 3D-T1-wi sequence to look for global or focal atrophy. The parameters of

199 acquisitions were as follows. The DTI sequence consisted in dual echo-planar

200 imaging: 40 axial slices; repetition time, 12000 ms; echo time, 100.9 ms; slice

201 thickness, 3.5 mm; matrix, 160x160; field of view, 24 cmx24 cm; b values, 0 and 1000

202 s/mm² applied in 32 non-collinear directions. The 3D-T1 was an inversion recovery

203 gradient echo sequence: 288 slices; repetition time, 11.4 ms; echo time, 4.3 ms;

204 inversion time, 400 ms; flip angle, 15°; slice thickness, 0.8 mm; matrix, 384x384; field

205 of view, 25 cmx25 cm.

206

207 **Image Processing**

208 **Measurement of DTI metrics along the optic radiations**

209 From the DTI data, the distortions induced by eddy currents were first corrected, then

210 a diffusion tensor model was fitted at each voxel using Olea Medical® software to

211 generate fractional anisotropy (FA) maps and to investigate the microstructural

212 integrity of the optic radiations. The optic radiations were identified using deterministic

213 tractography between two seed-regions of interest (ROIs) over the proximal and distal

214 optic radiations according to previously published method and landmarks[29]. The

215 proximal ROI was placed near the lateral geniculate nuclei, while the distal ROI was

216 placed just anterior to its termination in the visual cortex. Fiber tract propagation was

217 terminated for FA<0.2 and angle<35° based on agreed-upon thresholds. ROIs were

218 placed by a specialized neuroradiologist symetrically, based on color-coded FA maps

219 and trace DTI images on the anterior and posterior part of the expected pathway of the

220 optic radiations (green boxes on Figure 1). Fibers whose directions did not correspond

221 to the optic radiations based on anatomic knowledge and DTI-derived atlas were

222 excluded by adding additional ROIs and a logical "not" function[30] (red boxes on Figure

223 1). Only fibers that connected the anterior and posterior regions of interest were

224 selected for further analysis. The analysis was independently repeated for a subset of

225 cases (n=25 out of the 100 cases) by a specialized ophthalmologist with an inter-

226 reader agreement of 0.88.

227 The median FA and its sub-component (axial and radial diffusivity, AD and RD

228 respectively) as well as the mean diffusivity were measured along the reconstructed

229 optic radiations (green streamlines on Figure 1). Decreased FA and increased MD

230 values is usually considered as a proxy of axonal disruption[31].

231 None of the people participating in FA measurements had any access to the

232 case/control status of the participants, nor to any other clinical data.

233

234 **MRI volumetric measurements**

235 For volumetric analyses, T1-weighted images were processed using the volBrain

236 system (http://volbrain.upv.es). After denoising[32], images were affine-registered[33] into

237 the Montreal Neurological Institute space and the total brain volume was estimated

238 using the Nonlocal Intracranial Cavity Extraction method[34]. Hippocampus was

239 segmented using patch-based multi-template approach[35] following the international

240 consortium from the EADC-ADNI Harmonized Protocol for anatomical definitions of the

241 hippocampus[36]. To control variations in head size between subjects, total brain

242 volumes and hippocampal volumes were scaled using the volumetric scaling factor

243 determined through the affine registration to the MNI brain template.

244

For DTI analysis within the hippocampus masks, an in-house pipeline (dtiBrain) was used to process diffusion-weighted images. First, diffusion-weighted images were affine-registered to the T1w MRI in the MNI space[32]. Then, to compensate for EPI distortion, a non-rigid registration was performed. Finally, a diffusion tensor model was fitted at each voxel using FSL 5.031 (fmrib.ox.ac.uk/fsl), generating FA and MD maps. Mean FA and MD were measured within the hippocampal masks previously generated on anatomical T1-weighted MRI.

252

Statistical analysis

Statistical analysis was performed using SAS 9.3 (SAS Institute Inc, Cary, NC).

Differences of MRI characteristics between glaucoma subjects and healthy controls were tested using logistic conditional analyses, for parameters both along optic radiations and outside the visual pathway (globally for white and grey matter and in hippocampal and amygdala structures). Additionally, within the group of patients with glaucoma, we used mixed linear regression analyses, adjusted for sex and age (as a continuous variable expressed in years), to test the associations between optic radiation DTI parameters (FA, MD, AD, RD) and the parameters of severity of the disease (VCDR, mean deviation of VF and RNFL). This type of analysis allows taking into account both right and left sides of each patient, while taking into account the intra-individual correlation between sides. In particular, this allowed studying the associations of ocular parameters with homolateral (right optic radiation with right eye and left with left eye) and contralateral (right optic radiation with left eye and vice versa) optic radiations MRI parameters. In these regression analyses, both ocular and

268 brain parameters were entered as z-scores. In addition, for RNFL, we also adjusted for

269 axial length, which is strongly associated with RNFL[37].

270

271 **RESULTS**

272 **Demographic and ophthalmological characteristics**

273 As shown in Table 1, cases and controls were similar for age, gender, history of

274 cardiovascular diseases or risk factors and MMSE. Family history of glaucoma was

275 reported by 58 % of glaucoma patients, and 0 % of controls (since this was an

276 exclusion criterion for controls).

277 As shown in Table 2, cases and controls did not significantly differ for visual acuity

278 (distance and near), intraocular pressure and axial length. As expected, they were

279 significantly different for central corneal thickness, VCDR, RNFL thickness and visual

280 field parameters. Similar results were observed for the left eye (Table 3).

281 In our study, 70% of glaucoma patients had an early stage of the disease, 20% a

282 moderate stage and 10% an advanced or severe stage, according to the Hodapp-

283 Parrish-Anderson classification.

284

285 **Comparison of MRI parameters along optic radiations between glaucoma and**

286 **control subjects**

287 One patient refused to do MRI examination and 3 MRI examinations were insufficient

288 quality for analysis, leaving 49 glaucoma patients and 47 controls for the comparison

289 of MRI parameters (Table 4). The optic radiations were similarly reconstructed for

290 glaucoma and control subjects (similar length and volume and reconstructed

291 streamlines). Glaucoma patients showed significantly lower FA along the optic

292 radiations than controls (0.57 vs 0.59, p=0.02), which was driven by significant

293 increase in radial diffusivity (52.8 10^{-5} mm^2/s vs 49.7 10^{-5} mm^2/s, p=0.03) while axial

294 diffusivity was unchanged. Mean diffusivity tended to be slightly higher in glaucoma

295 patients, but this did not reach statistical significance (82.4 10^{-5} mm^2/s vs 80.6 10^{-5}

296 mm^2/s p=0.10).

297

298
299 **Associations of homo- and contralateral optic radiation parameters with the**

300 **severity of the disease in glaucoma patients**

301 Table 5 shows the associations of optic radiation parameters (FA, MD, RD and AD)

302 with the ophthalmological parameters of glaucoma severity evaluated by visual field,

303 optic disc cupping and RNFL thickness, only among patients with glaucoma (n=50).

304 We tested associations of ophthalmological parameters with MRI parameters on the

305 homolateral (right eye – right optic radiation and left eye – left optic radiation) and

306 contralateral (right-left and left-right) sides. For the homolateral side, significant

307 associations were found between optic radiations FA and mean deviation of the visual

308 field (β= -0.22; p= 0.03), VCDR (β= -0.42; p= 0.0003) and RNFL (β= 0.22; p= 0.03).

309 The direction of the association is opposite for RNFL, since RNFL decreases with

310 higher severity of glaucoma, while other parameters increase with severity. Mean and

311 radial diffusivities increased with the severity of the disease measured by VCDR,

312 (p<0.006 and p<0.0008, respectively), but were not significantly associated with mean

313 deviation of VF or RNFL thickness. By contrast, axial diffusivity, as well as length and

314 volume of optic radiations were not significantly associated with any of the severity

315 parameters.

316 With regard to the contralateral side, associations of MRI parameters with glaucoma

317 severity parameters were much weaker, and reached statistical significance only for

318 the association of FA and RD with VCDR (p=0.01 and p=0.02, respectively).

319

Brain volumes analyses between cases and controls

321 Finally, we did not evidence any statistically significant difference between glaucoma

322 subjects and controls for volumes and DTI parameters of cerebrum white and grey

323 matters, hippocampus and amygdala (Table 6).

324

325

DISCUSSION

327 Our study demonstrates microstructural changes of the optic radiations in glaucoma,

328 as evaluated by lower FA driven by higher RD, and a correlation between the level of

329 structural modifications and disease severity.

330 Using MRI at 1.5T[38] or 3T[25,26,39] a few case-control studies have also reported such

331 modifications of diffusion parameters in optic radiations of glaucoma patients. All these

332 studies found significantly lower FA in glaucoma patients compared with control

333 patients. In the present study, which included 70 % of early stages of glaucoma, FA

334 differences between cases and controls are numerically small (about 0.02 for a mean

335 of about 0.60, i.e about 3.3 %). However, the standard deviation is also small (about

336 0.04), showing low inter-individual variability in this parameter, and the difference is

337 substantial when related to the standard deviation (about 0.5 SD), suggesting a major

338 effect of glaucoma on this highly conserved parameter. In other studies, the

339 differences in FA of optic radiations observed between glaucoma patients and controls

340 were larger, but these studies generally included more severe cases. The study by

341 Engelhorn et al included 22 severe glaucoma cases, and observed a difference in FA

342 of optic radiations ranging from 17 % to 30 % according to the localization (anterior,

343 central, posterior)[39]. The study by Murai et al included 18 severe glaucoma cases, 9

344 moderate and only 2 mild, and observed a 14 % difference in FA of the optic

345 radiations[38]. The study by Garaci et al included 4 pre-perimetric glaucoma cases, 4

346 early, 4 moderate and 4 severe cases and observed a 36 % differences in FA of the

347 optic radiations[25]. Finally, the study by Chen et al included a majority of severe cases

348 (36 eyes with MD>9.5 dB out of 50) but did not report numerically the averages of

349 optic radiations FA[26].

350 Furthermore, we observed higher RD value in glaucoma patients and its correlation

351 with disease severity whereas AD was not significantly different between glaucoma

352 and control patients. Although, AD and RD are the two components of FA, these

353 parameters have been scarcely analyzed in the literature and some studies have

354 already reported increasing RD in glaucoma subjects compared to controls[24].

355 Even though the underlying pathological alterations are not specifically known, animal

356 studies have suggested that higher RD could mainly represent myelin loss while lower

357 AD could be a more specific marker of neuronal loss. However these considerations

358 were based on simplistic models and whether alterations of optic radiations truly

359 predominate on myelin or axon component cannot be formally ascertained for

360 glaucoma patients, for whom other modifications such as microglia activation may

361 confound the data.

362 Additionally, we observed a trend towards higher mean diffusivity value in the

363 glaucoma group without reaching statistical significance. However, we observed a

364 significant positive correlation between mean diffusivity and disease severity

365 measured with VCDR. Two studies also showed higher mean diffusivity in glaucoma

366 patients[25,26]. While FA measures the degree of cellular structural alignment within fiber

367 tracts and their structural integrity, mean diffusivity measures the average motion of

368 water molecules independently of fiber directionality and is considered as an additional

369 marker of axonal disruption. As these studies included patients with advanced

370 glaucoma, our findings might be explained by a lack of statistical power and a lower

371 grade of disease severity in our glaucoma group. Such converging evidence of loss of

372 fiber integrity in optic radiations in glaucoma cannot be measured in terms of length

373 and volume of the optic radiations, which were similar in both groups probably

374 because our measurements were made prior to fiber loss or major disorganization.

375

376 We also observed an association of diffusivity parameters (mainly FA and RD), with

377 the severity of glaucoma (assessed by mean deviation of the visual field, VCDR and

378 RNFL measured with SD-OCT), suggesting that microstructural changes to the optic

379 radiations is one of the components of the severity that could participate in the

380 clinical status of the patients and the alteration of the visual field. Although we mainly

381 included early and moderate glaucoma as defined by the Hodapp-Parrish-Anderson

382 classification, our findings are consistent with some previous studies, which included

383 more advanced cases[26,38–40]. All these studies also evidenced significant

384 associations of optic radiations FA with structural parameters of optic nerve head

385 degeneration evaluated with VCDR or time-domain RNFL thickness, as well as

386 functional visual field alterations. For example, Michelson *et al.* found a correlation

387 between FA and visual field[40]. Thus, all these results illustrate the fact that FA could

388 be a strong biomarker of glaucoma severity.

389 Our study also assessed the associations of glaucoma severity according to FA of

390 homolateral and contralateral optic radiations. Interestingly, glaucoma severity

391 parameters – in particular VCDR – were more strongly associated with homolateral

392 optic radiations diffusion parameters than with contralateral parameters. As chiasmatic

393 decussation of optic pathways results in approximately 50% crossing of axons on the

394 contralateral side[41], we would expect similar associations of glaucoma severity

395 parameters with homolateral and contralateral diffusion parameters. However, our

396 findings might also be related to an increased vulnerability of some specific retinal

397 nerve fiber bundles of the optic nerve head resulting in an atrophy of optic radiations

398 more predominant on the homolateral side of the decussation than on the

399 controlateral. Indeed, several studies have demonstrated a specific vulnerability of the

400 temporal and temporal-inferior sides of the optic nerve head to glaucoma damage[42–44].

401 Thus, we could expect an increased atrophy of the corresponding optic radiation

402 predominant on the homolateral side that could explain our findings. However, even if

403 temporal and temporal-inferior nerve fiber layers are more vulnerable to glaucomatous

404 damage, the meaning of our findings should be interpreted with caution and would

405 need further exploration to be confirmed and to identify the exact underlying

406 mechanism. Indeed, distribution of RNFL is not homogeneous around the optic nerve

407 head with superior and inferior sectorial RNFL thicker than nasal or temporal RNFL

408 sectors. Furthermore the mean optic disc-fovea angle deliminating superior and

409 inferior nerve fiber layers, is around $8°$[45]. Thus the exact distribution of nerve fiber

410 layers of the retina that decussates to the contralateral optic tract or remains on the

411 ipsilateral optic tract and finally leads to a vertical delimitation through the fovea on the

412 hemivisual field test remains unclear. Hence, in our study, the corresponding optic

413 radiations in the homo or contralateral side could not be accurately matched to specific

414 sectors of the retina or the optic nerve head.

415 Although high intraocular pressure is the main risk factor of glaucoma, this disease is

416 increasingly considered as a neuro-ophthalmological and neurodegenerative

417 disease[46]. Furthermore, there are still controversies on the association between

418 glaucoma and some other neurodegenerative diseases as Alzheimer's disease. In

419 particular, in a cohort of elderly subjects followed every 2 years, we observed an

420 association of POAG with incident dementia[19]. Volume changes beyond the visual

421 system in glaucoma patients have also been reported in several studies but with

422 inconsistent results. For instance, Frezzotti *et al.* reported that POAG patients had

423 brain atrophy in some grey matter regions and the visual cortex[21]. By contrast,

424 Williams *et al.* found five cerebral structures larger in the glaucoma group than in the

425 control group[22]. Chen *et al.* revealed both a decreasing grey matter volume in some

426 regions and an increasing grey matter volume in some others[14]. In the present study,

427 we analyzed brain globally and focused on brain regions that are well known to be

428 affected in the course of Alzheimer's disease – particularly hippocampus – and did not

429 evidence any significant difference for any of the studied regions of interest, neither in

430 volume nor in parameters of diffusivity. However, as we included subjects with MMSE

431 ≥26 at baseline, the risk of brain structures atrophy was probably limited. Regarding

432 the hippocampus, results have been particularly inconsistent, since Frezzotti *et al.*

433 reported decreased hippocampus volume in glaucoma patients[21], while Williams *et al.*

434 reported no significant difference of hippocampus volume between glaucoma and

435 controls, but an increase in hippocampus volume with disease severity in patients with

436 glaucoma[22].

437 Such differences between study results may be explained by differences in study

438 methodology, in particular regarding the selection of subjects and severity of the

439 disease, MRI sequences used or definition of regions of interest. For instance, in a

440 recent study by Frezzotti et al, only severe cases of glaucoma (but not early) showed

441 grey matter atrophy of the visual cortex and hippocampus[47]. The evolution of brain

442 volume in the course of glaucoma and its association with other neurodegenerative

443 diseases would need further investigation and prospective follow-up of subjects.

444 Finally, functional MRI may offer new insights into the brain modifications associated

445 with glaucoma, as suggested by two recent studies, showing functional modifications

446 of the visual cortex at the earliest stages of the disease[47,48].

447

448

449 In conclusion, we confirmed microstructural changes of optic radiations in glaucoma

450 and its association with glaucoma severity. In accordance with several other studies,

451 DTI appears as an objective measurement for evaluating alterations of the visual

452 pathways in glaucoma and provides new insight in the pathophysiological process of

453 glaucoma. A prospective evaluation of our cohort of patients would be of interest to

454 observe the evolution of these microstructural modifications of optic radiations and to

455 analyze the evolution of brain volume in association with the evolution of glaucoma

456 disease. DTI could represent a future way to explore central nervous system of

457 glaucomatous subjects, leading to a better understanding of the pathophysiology and,

458 potentially, to help clinical trials evaluate new therapeutic strategies based on

459 neuroprotection or brain repair.

460

461

462 **REFERENCES**

463

464 1.   Resnikoff S, Pascolini D, Etya'ale D, et al. Global data on visual impairment in
465 the year 2002. *Bull World Health Organ*. 2004;82(11):844-851. doi:/S0042-
466 96862004001100009.
467 2.   Tham Y-C, Li X, Wong TY, Quigley HA, Aung T, Cheng C-Y. Global
468 prevalence of glaucoma and projections of glaucoma burden through 2040: a
469 systematic review and meta-analysis. *Ophthalmology*. 2014;121(11):2081-2090.
470 doi:10.1016/j.ophtha.2014.05.013.
471 3.   Weinreb RN, Khaw PT. Primary open-angle glaucoma. *Lancet*.
472 2004;363(9422):1711-1720. doi:10.1016/S0140-6736(04)16257-0.
473 4.   O'Hare F, Rance G, McKendrick AM, Crowston JG. Is primary open-angle
474 glaucoma part of a generalized sensory neurodegeneration? A review of the
475 evidence. *Clin Experiment Ophthalmol*. 2012;40(9):895-905. doi:10.1111/j.1442-

476   9071.2012.02812.x.
477   5.   Gupta N, Yücel YH. Glaucoma as a neurodegenerative disease. *Curr Opin*
478   *Ophthalmol*. 2007;18(2):110-114. doi:10.1097/ICU.0b013e3280895aea.
479   6.   Yucel YH, Gupta N. A framework to explore the visual brain in glaucoma with
480   lessons from models and man. *Exp Eye Res*. 2015;141:171-178.
481   doi:10.1016/j.exer.2015.07.004.
482   7.   Yücel Y. Central nervous system changes in glaucoma. *J Glaucoma*. 2013;22
483   Suppl 5:S24-25. doi:10.1097/IJG.0b013e3182934a55.
484   8.   Zhang S, Wang H, Lu Q, et al. Detection of early neuron degeneration and
485   accompanying glial responses in the visual pathway in a rat model of acute
486   intraocular hypertension. *Brain Res*. 2009;1303:131-143.
487   doi:10.1016/j.brainres.2009.09.029.
488   9.   Boucard CC, Hernowo AT, Maguire RP, et al. Changes in cortical grey matter
489   density associated with long-standing retinal visual field defects. *Brain J Neurol*.
490   2009;132(Pt 7):1898-1906. doi:10.1093/brain/awp119.
491   10.   Gupta N, Ang L-C, Noël de Tilly L, Bidaisee L, Yücel YH. Human glaucoma
492   and neural degeneration in intracranial optic nerve, lateral geniculate nucleus, and
493   visual cortex. *Br J Ophthalmol*. 2006;90(6):674-678. doi:10.1136/bjo.2005.086769.
494   11.   Gupta N, Greenberg G, de Tilly LN, Gray B, Polemidiotis M, Yücel YH.
495   Atrophy of the lateral geniculate nucleus in human glaucoma detected by magnetic
496   resonance imaging. *Br J Ophthalmol*. 2009;93(1):56-60.
497   doi:10.1136/bjo.2008.138172.
498   12.   Zhang YQ, Li J, Xu L, et al. Anterior visual pathway assessment by magnetic
499   resonance imaging in normal-pressure glaucoma. *Acta Ophthalmol (Copenh)*.
500   2012;90(4):e295-302. doi:10.1111/j.1755-3768.2011.02346.x.
501   13.   Zikou AK, Kitsos G, Tzarouchi LC, Astrakas L, Alexiou GA, Argyropoulou MI.
502   Voxel-based morphometry and diffusion tensor imaging of the optic pathway in
503   primary open-angle glaucoma: a preliminary study. *AJNR Am J Neuroradiol*.
504   2012;33(1):128-134. doi:10.3174/ajnr.A2714.
505   14.   Chen WW, Wang N, Cai S, et al. Structural Brain Abnormalities in Patients
506   with Primary Open-Angle Glaucoma: A Study with 3T MR Imaging. *Investig*
507   *Opthalmology Vis Sci*. 2013;54(1):545. doi:10.1167/iovs.12-9893.
508   15.   Dai H, Mu KT, Qi JP, et al. Assessment of lateral geniculate nucleus atrophy
509   with 3T MR imaging and correlation with clinical stage of glaucoma. *AJNR Am J*
510   *Neuroradiol*. 2011;32(7):1347-1353. doi:10.3174/ajnr.A2486.
511   16.   Chan KC, Fu Q, Hui ES, So K, Wu EX. Evaluation of the retina and optic nerve
512   in a rat model of chronic glaucoma using in vivo manganese-enhanced magnetic
513   resonance imaging. *NeuroImage*. 2008;40(3):1166-1174.
514   doi:10.1016/j.neuroimage.2008.01.002.
515   17.   Chan KC, So K, Wu EX. Proton magnetic resonance spectroscopy revealed
516   choline reduction in the visual cortex in an experimental model of chronic glaucoma.
517   *Exp Eye Res*. 2009;88(1):65-70. doi:10.1016/j.exer.2008.10.002.
518   18.   Ho LC, Wang B, Conner IP, et al. In Vivo Evaluation of White Matter Integrity
519   and Anterograde Transport in Visual System After Excitotoxic Retinal Injury With
520   Multimodal MRI and OCT. *Invest Ophthalmol Vis Sci*. 2015;56(6):3788-3800.
521   doi:10.1167/iovs.14-15552.
522   19.   Helmer C, Malet F, Rougier M-B, et al. Is there a link between open-angle
523   glaucoma and dementia?: The Three-City-Alienor Cohort. *Ann Neurol*. May 2013.
524   doi:10.1002/ana.23926.
525   20.   Lin I-C, Wang Y-H, Wang T-J, et al. Glaucoma, Alzheimer's disease, and

526 Parkinson's disease: an 8-year population-based follow-up study. *PloS One*.
527 2014;9(9):e108938. doi:10.1371/journal.pone.0108938.
528 21.   Frezzotti P, Giorgio A, Motolese I, et al. Structural and functional brain
529 changes beyond visual system in patients with advanced glaucoma. *PloS One*.
530 2014;9(8):e105931. doi:10.1371/journal.pone.0105931.
531 22.   Williams AL, Lackey J, Wizov SS, et al. Evidence for widespread structural
532 brain changes in glaucoma: a preliminary voxel-based MRI study. *Invest Ophthalmol*
533 *Vis Sci*. 2013;54(8):5880-5887. doi:10.1167/iovs.13-11776.
534 23.   Le Bihan D, Iima M. Diffusion Magnetic Resonance Imaging: What Water Tells
535 Us about Biological Tissues. *PLoS Biol*. 2015;13(7):e1002203.
536 doi:10.1371/journal.pbio.1002203.
537 24.   El-Rafei A, Engelhorn T, Wärntges S, Dörfler A, Hornegger J, Michelson G. A
538 framework for voxel-based morphometric analysis of the optic radiation using
539 diffusion tensor imaging in glaucoma. *Magn Reson Imaging*. 2011;29(8):1076-1087.
540 doi:10.1016/j.mri.2011.02.034.
541 25.   Garaci FG, Bolacchi F, Cerulli A, et al. Optic nerve and optic radiation
542 neurodegeneration in patients with glaucoma: in vivo analysis with 3-T diffusion-
543 tensor MR imaging. *Radiology*. 2009;252(2):496-501.
544 doi:10.1148/radiol.2522081240.
545 26.   Chen Z, Lin F, Wang J, et al. Diffusion tensor magnetic resonance imaging
546 reveals visual pathway damage that correlates with clinical severity in glaucoma. *Clin*
547 *Experiment Ophthalmol*. 2013;41(1):43-49. doi:10.1111/j.1442-9071.2012.02832.x.
548 27.   Folstein MF, Folstein SE, McHugh PR. "Mini-mental state". A practical method
549 for grading the cognitive state of patients for the clinician. *J Psychiatr Res*.
550 1975;12(3):189-198.
551 28.   Maeda N, Klyce SD, Smolek MK, Thompson HW. Automated keratoconus
552 screening with corneal topography analysis. *Invest Ophthalmol Vis Sci*.
553 1994;35(6):2749-2757.
554 29.   Reich DS, Smith SA, Gordon-Lipkin EM, et al. Damage to the optic radiation in
555 multiple sclerosis is associated with retinal injury and visual disability. *Arch Neurol*.
556 2009;66(8):998-1006. doi:10.1001/archneurol.2009.107.
557 30.   Wakana S, Jiang H, Nagae-Poetscher LM, van Zijl PCM, Mori S. Fiber tract-
558 based atlas of human white matter anatomy. *Radiology*. 2004;230(1):77-87.
559 doi:10.1148/radiol.2301021640.
560 31.   Wheeler-Kingshott C a. M, Trip SA, Symms MR, Parker GJM, Barker GJ,
561 Miller DH. In vivo diffusion tensor imaging of the human optic nerve: pilot study in
562 normal controls. *Magn Reson Med*. 2006;56(2):446-451. doi:10.1002/mrm.20964.
563 32.   Manjón JV, Coupé P, Martí-Bonmatí L, Collins DL, Robles M. Adaptive non-
564 local means denoising of MR images with spatially varying noise levels. *J Magn*
565 *Reson Imaging JMRI*. 2010;31(1):192-203. doi:10.1002/jmri.22003.
566 33.   Avants BB, Tustison NJ, Song G, Cook PA, Klein A, Gee JC. A reproducible
567 evaluation of ANTs similarity metric performance in brain image registration.
568 *NeuroImage*. 2011;54(3):2033-2044. doi:10.1016/j.neuroimage.2010.09.025.
569 34.   Manjón JV, Eskildsen SF, Coupé P, Romero JE, Collins DL, Robles M.
570 Nonlocal intracranial cavity extraction. *Int J Biomed Imaging*. 2014;2014:820205.
571 doi:10.1155/2014/820205.
572 35.   Coupé P, Manjón JV, Fonov V, Pruessner J, Robles M, Collins DL. Patch-
573 based segmentation using expert priors: application to hippocampus and ventricle
574 segmentation. *NeuroImage*. 2011;54(2):940-954.
575 doi:10.1016/j.neuroimage.2010.09.018.

576 36. Frisoni GB, Jack CR, Bocchetta M, et al. The EADC-ADNI Harmonized
577 Protocol for manual hippocampal segmentation on magnetic resonance: evidence of
578 validity. *Alzheimers Dement J Alzheimers Assoc.* 2015;11(2):111-125.
579 doi:10.1016/j.jalz.2014.05.1756.
580 37. Sowmya V, Venkataramanan VR, Prasad V. Effect of Refractive Status and
581 Axial Length on Peripapillary Retinal Nerve Fibre Layer Thickness: An Analysis Using
582 3D OCT. *J Clin Diagn Res JCDR.* 2015;9(9):NC01-04.
583 doi:10.7860/JCDR/2015/14112.6480.
584 38. Murai H, Suzuki Y, Kiyosawa M, Tokumaru AM, Ishii K, Mochizuki M. Positive
585 correlation between the degree of visual field defect and optic radiation damage in
586 glaucoma patients. *Jpn J Ophthalmol.* February 2013. doi:10.1007/s10384-013-0233-
587 0.
588 39. Engelhorn T, Michelson G, Waerntges S, et al. A new approach to assess
589 intracranial white matter abnormalities in glaucoma patients: changes of fractional
590 anisotropy detected by 3T diffusion tensor imaging. *Acad Radiol.* 2012;19(4):485-
591 488. doi:10.1016/j.acra.2011.12.005.
592 40. Michelson G, Engelhorn T, Wärntges S, El Rafei A, Hornegger J, Doerfler A.
593 DTI parameters of axonal integrity and demyelination of the optic radiation correlate
594 with glaucoma indices. *Graefes Arch Clin Exp Ophthalmol Albrecht Von Graefes
595 Arch Für Klin Exp Ophthalmol.* 2013;251(1):243-253. doi:10.1007/s00417-011-1887-
596 2.
597 41. Pietrasanta M, Restani L, Caleo M. The Corpus Callosum and the Visual
598 Cortex: Plasticity Is a Game for Two. *Neural Plast.* 2012;2012:1-10.
599 doi:10.1155/2012/838672.
600 42. Strouthidis NG, Fortune B, Yang H, Sigal IA, Burgoyne CF. Longitudinal
601 change detected by spectral domain optical coherence tomography in the optic nerve
602 head and peripapillary retina in experimental glaucoma. *Invest Ophthalmol Vis Sci.*
603 2011;52(3):1206-1219. doi:10.1167/iovs.10-5599.
604 43. Tan O, Chopra V, Lu AT-H, et al. Detection of macular ganglion cell loss in
605 glaucoma by Fourier-domain optical coherence tomography. *Ophthalmology.*
606 2009;116(12):2305-2314.e1-2. doi:10.1016/j.ophtha.2009.05.025.
607 44. Yang Y, Zhang H, Yan Y, Gui Y, Zhu T. Comparison of optic nerve
608 morphology in eyes with glaucoma and eyes with non-arteritic anterior ischemic optic
609 neuropathy by Fourier domain optical coherence tomography. *Exp Ther Med.*
610 2013;6(1):268-274. doi:10.3892/etm.2013.1115.
611 45. Jonas RA, Wang YX, Yang H, et al. Optic Disc - Fovea Angle: The Beijing Eye
612 Study 2011. *PloS One.* 2015;10(11):e0141771. doi:10.1371/journal.pone.0141771.
613 46. Chang EE, Goldberg JL. Glaucoma 2.0: Neuroprotection, Neuroregeneration,
614 Neuroenhancement. *Ophthalmology.* 2012;119(5):979-986.
615 doi:10.1016/j.ophtha.2011.11.003.
616 47. Murphy MC, Conner IP, Teng CY, et al. Retinal Structures and Visual Cortex
617 Activity are Impaired Prior to Clinical Vision Loss in Glaucoma. *Sci Rep.*
618 2016;6:31464. doi:10.1038/srep31464.
619 48. Frezzotti P, Giorgio A, Toto F, De Leucio A, De Stefano N. Early changes of
620 brain connectivity in primary open angle glaucoma. *Hum Brain Mapp.* August 2016.
621 doi:10.1002/hbm.23330.
622
623

Figure 1. Building of optic radiations and measurement of fractional anisotropy, using the Olea Medical [R] software (image: CHU de Bordeaux, department of neuroimaging).

Green boxes are the markers placed manually on anterior and posterior parts of the optic radiations. Green lines are optic radiations automatically reconstructed by the Olea Medical[®] software. Red boxes are markers manually placed to manually deleted fibers outside the expected area.
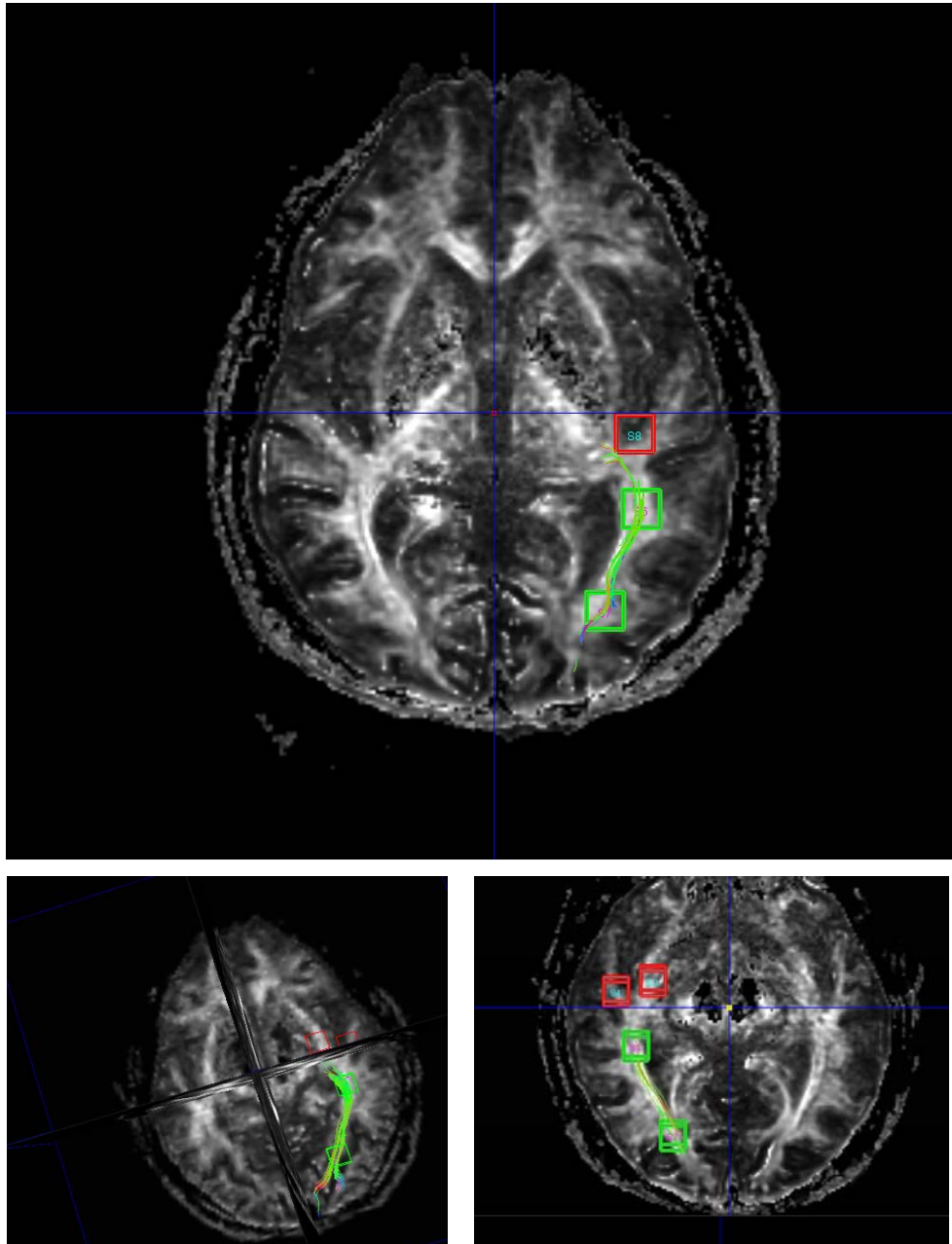
Table 1: General characteristics

Characteristics	Glaucoma (n=50)	Control (n=50)	p-value*
Age (years, mean(SD))	61.9 (6.9)	61.9 (7.0)	0.98
Sex (n, %)			1
Male	20 (40)	20 (40)	
Female	30 (60)	30 (60)	
MMSE (mean(SD))	29.3 (0.8)	29.4 (0.8)	0.7
Family history of glaucoma (n (%))			<0.0001
Yes	29 (58)	0 (0)	
No	16 (32)	50 (100)	
Unknown	5 (10)	0 (0)	
Self-reported medical history			
Hypertension (n (%))	11 (22)	12 (24)	0.81
Hypercholesterolemia (n (%))	14 (28)	12 (24)	0.65
Hypertriglyceridemia (n (%))	2 (4)	3 (6)	0.65
Myocardial infarction (n (%))	2 (4)	1 (2)	0.56
Smoking (n (%))			0.67
Never	29 (58)	25 (50)	
Former	17 (34)	19 (38)	
Current	4 (8)	6 (12)	

MMSE: Mini Mental State Examination
* Chi-square for categorical variables and Student t-test for continuous variables

Table 2: Ophthalmological characteristics; right eye (mean (standard deviation))

Characteristics	Glaucoma (n=50)	Control (n=50)	p-value*
Best-Corrected Visual Acuity (logMAR)			
Distance	0.03 (0.09)	0.006 (0.02)	0.09
Near	0.19 (0.07)	0.18 (0.00)	0.2
Central corneal thickness (µm)	525.9 (30.9)	544.0[1] (31.9)	0.005
Axial Length (mm)	24.1 (1.1)	23.7 (1.2)	0.15
IOP (mmHg)	14.6 (3.7)	14.7 (2.5)	0.82
Vertical Cup : Disc Ratio	0.8 (0.2)[1]	0.3 (0.2)[1]	<0.0001
RNFL Thickness (µm)	76.9 (17.7)	93.2 (9.9)	<0.0001
Visual field (dB)			
Mean Sensitivity	21.9 (6.1)	26.6 (1.1)	<0.0001
Mean Deviation	5.0 (6.0)	0.3 (1.0)	<0.0001
Loss Variance	22.6 (26.3)	5.0 (1.8)	<0.0001

RNFL: Retinal Nerve Fiber Layer

IOP: Intraocular Pressure

* Chi-square for categorical variables and Student t-test for continuous variables

[1] One missing data

Table 3: Ophthalmological characteristics; left eye (mean (standard deviation))

Characteristics	Glaucoma (n=50)	Control (n=50)	p-value*
Best-Corrected Visual Acuity (logMAR)			
Far	0.03 (0.08)	0.006 (0.02)	0.08
Near	0.2 (0.1)	0.2 (0)	0.1
Central corneal thickness (µm)	524.6 (30.0)[1]	542.9 (28.4)[2]	0.003
Axial Length (mm)	24.0 (1.0)	23.5 (0.8)	0.003
IOP (mmHg)	14.2 (3.2)	15.2 (2.4)	0.09
Vertical Cup : Disc Ratio			
Funduscopy	0.8 (0.2)	0.3 (0.2)	<0.0001
RNFL Thickness (µm)	70.1 (18.7)	93.1 (9.7)	<0.0001
Visual field (dB)			
Mean Sensitivity: MS	21.8 (4.6)	26.6 (1.2)	<0.0001
Mean Deviation: MD	5.1 (4.5)	0.3 (1.1)	<0.0001
Loss Variance: LV	28.1 (28.0)	4.7 (2.2)	<0.0001

RNFL: Retinal Nerve Fiber Layer

IOP: Intraocular Pressure

* Chi-square for categorical variables and Student t-test for continuous variables

[1] One missing data [2] Two missing data

Table 4: Comparison of MRI parameters along optic radiations between glaucoma and control subjects (mean (standard deviation))

	Glaucoma (n=49)	Control (n=47)	P-value*
Fractional anisotropy	0.57 (0.04)	0.59 (0.03)	0.02
Mean diffusivity (10^{-5} mm^2/s)	82.38 (6.43)	80.62 (4.87)	0.10
Axial diffusivity (10^{-5} mm^2/s)	141.59 (7.14)	142.37 (6.74)	0.53
Radial diffusivity (10^{-5} mm^2/s)	52.78 (6.74)	49.74 (5.04)	0.03
Length (mm)	63.91 (6.80)	63.72 (7.15)	0.74
Volume (cm^3)	20.79 (9.13)	24.96 (12.33)	0.11

*P-value: logistic conditional analyses

Table 5: Associations of homo- and contra-lateral optic radiation parameters with the severity of the disease in glaucoma patients

	Visual field Mean Deviation		Funduscopy Vertical Cup/Disc Ratio		SD-OCT examination RNFL thickness	
	β[95%CI]	P	β [95%CI]	P	β [95%CI]	P
Homolateral						
Fractional anisotropy	-0.22 [-0.41;-0.02]	**0.03**	-0.42 [-0.64;-0.21]	**0.0003**	0.22 [0.03;0.41]	**0.03**
Mean diffusivity	0.02 [-0.17;0.21]	0.80	0.29 [0.08;0.50]	**0.008**	-0.15 [-0.34;0.04]	0.12
Axial diffusivity	-0.11 [-0.31;0.08]	0.26	0.09 [-0.14;0.31]	0.45	-0.06 [-0.26;0.14]	0.56
Radial diffusivity	0.09 [-0.10;0.28]	0.33	0.38 [0.17;0.59]	**0.0006**	-0.18 [-0.37;-0.007]	0.06
Controlateral						
Fractional anisotropy	-0.17 [-0.37;0.02]	0.09	-0.28 [-0.55;-0.06]	**0.01**	0.10 [-0.09;0.30]	0.30
Mean diffusivity	0.13 [-0.06;0.31]	0.19	0.20 [-0.02;0.41]	0.07	0.01 [-0.18;0.21]	0.91
Axial diffusivity	0.04 [-0.15;0.24]	0.67	0.07 [-0.16;0.30]	0.55	0.09 [-0.11;0.30]	0.34
Radial diffusivity	0.15 [-0.04;0.34]	0.11	0.25 [0.04;0.46]	**0.02**	-0.03 [-0.23;0.16]	0.72

CI: Confidence Interval; RNFL: Retinal Nerve Fiber Layer
P-value adjusted for age and gender, with additional adjustment for axial length for RNFL

Table 6: Comparison of DTI parameters and MRI-based volume between glaucoma and control subjects (mean (standard deviation))

	Cerebrum white matter			Cerebrum grey matter			Hippocampus			Amygdala		
	Glaucoma	Control	P-value*	Glaucoma	Control	P-value	Glaucoma	Control	P-value	Glaucoma	Control	P-value
	(n=48)	(n=48)		(n=48)	(n=48)		(n=48)	(n=48)		(n=48)	(n=48)	
Volume (cm^3)	275.28 (115.61)	238.25 (59.03)	0.06	270.19 (59.03)	283.09 (38.17)	0.18	3.95 (0.53)	3.84 (0.46)	0.16	0.60 (0.23)	0.55 (0.18)	0.22
DTI parameters	(n=41)	(n=41)		(n=41)	(n=41)		(n=41)	(n=41)		(n=41)	(n=41)	
FA	0.38 (0.02)	0.37 (0.02)	0.39	0.17 (0.01)	0.17 (0.01)	0.45	0.19 (0.01)	0.19 (0.02)	0.44	0.15 (0.02)	0.15 (0.01)	0.09
MD (10^{-5} mm^2/s)	78.34 (3.58)	78.19 (3.21)	0.79	121.70 (9.63)	120.01 (8.81)	0.25	98.83 (8.82)	97.72 (5.79)	0.42	80.45 (4.03)	80.56 (3.40)	0.87
AD (10^{-5} mm^2/s)	110.91 (2.80)	110.35 (2.53)	0.26	138.84 (10.50)	136.96 (9.67)	0.24	116.86 (9.78)	115.46 (6.17)	0.39	92.64 (4.43)	92.21 (3.31)	0.57
RD (10^{-5} mm^2/s)	62.24 (4.17)	62.27 (3.78)	0.96	113.20 (9.23)	111.60 (8.44)	0.26	90.02 (8.40)	88.90 (5.74)	0.44	74.35 (3.99)	74.73 (3.53)	0.57

Abreviations: AD: Axial diffusivity; FA: Fractional anisotropy; MD: Mean diffusivity; RD: Radial diffusivity

*P-value : logistic conditional analyses